Dynamics of Photosubstitution Reactions of Fe(CO) 5 : An Ultrafast Infrared Study of High Spin Reactivity

ARTICLE *in* JOURNAL OF THE AMERICAN CHEMICAL SOCIETY · JULY 2001

Impact Factor: 12.11 · DOI: 10.1021/ja010648r

Dynamics of Photosubstitution Reactions of $Fe(CO)_5$: An Ultrafast Infrared Study of High Spin Reactivity

Preston T. Snee, Christine K. Payne, Sheryl D. Mebane, Kenneth T. Kotz, and Charles B. Harris*

Contribution from the Department of Chemistry, University of California, Berkeley, California 94720, and Chemical Sciences Division, Ernest Orlando Lawrence Berkeley National Laboratory, Berkeley, California 94720

Received March 12, 2001

Abstract: The photosubstitution reactions of $Fe(CO)_5$ with alcohols and triethylphosphine have been studied in room temperature solution using femtosecond UV pump IR probe techniques. The dynamics of $Fe(CO)_5$ in alcohols show that the coordination of the hydroxyl group of the solvent with triplet $Fe(CO)_4$ is generally much faster than the coordination timescale observed with comparable singlet species. The physical reason for this is the fact that the metal C−H agostic bond is much weaker for triplets, thus allowing fast rearrangement to the hydroxyl group of the alcohol. In the case of triethylphosphine photosubstitution, the reaction is divided into parallel channels which include intersystem crossing and a spin conserving double carbonyl loss. The intermediates observed were studied using density functional theory (DFT) as well as ab initio quantum chemical calculations.

I. Introduction

While the photochemistry of $Fe(CO)_5$ has been extensively researched,[1−6] the ultrafast dynamics of the intermediate species remains a subject of debate in the literature. Recent studies of the photochemistry of $Fe(CO)_5$ in solution have shown that the primary photoproduct following excitation is triplet $^3Fe(CO)_4$.[7] To characterize the ultrafast dynamics of this high-spin intermediate, we have studied the concerted solvation/spin crossover of $^3Fe(CO)_4$ in a series of strong coupling solvents.[8] The general reactions under study are summarized in Scheme 1.

The formation of low-spin products from high-spin reactants is generally thought to be unfavorable due to intersystem crossing barriers. As a result, low-spin intermediate species should react faster than high-spin species as these additional barriers do not exist. However, it is possible that a high-spin intermediate may not react via the same mechanism as a singlet intermediate, possibly reversing this trend in the reaction rates. In our previous ligand rearrangement studies of coordinatively unsaturated singlet organometallic species in alcohols and in trialkylsilanes, it was found that a singlet σ-bonded alkyl solvate complex must dissociate to form the final product.[9] Corresponding studies with high-spin intermediates indicate that, unlike the singlet species, the triplet species coordinate weakly at best with the alkyl group of triethylsilane resulting in a much lower barrier for dissociation. Consequently, high-spin intermediates may react with the Si−H bond at a much faster rate.[1,7,10] These results are summarized in Scheme 2. To further explore the dynamics of high-spin organometallic intermediates, we have studied the triplet-to -singlet spin crossover/solvation reaction of $^3Fe(CO)_4$ in a series of alcohol solvents. These results are compared to the dynamics of the singlet intermediate $^1Cr(CO)_5$. A comparison of the singlet and triplet state reactivity demonstrates the importance of the solvent's structure and viscosity in the reactions of high-spin intermediates.

In addition to the above, a description of the photochemistry of $Fe(CO)_5$ would not be complete without some discussion of

Scheme 1. The Reactions of $Fe(CO)_5$ with Alcohol and Triethylphosphine

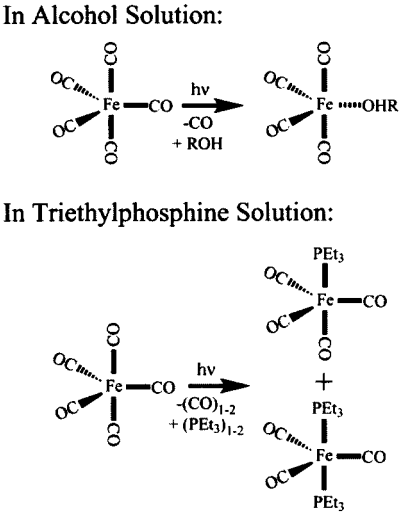

* To whom correspondence should be addressed.

(1) Poliakoff, M.; Turner, J. J. *J. Chem. Soc., Dalton Trans.* **1974**, 2276.
(2) Poliakoff, M.; Weitz, E. *Acc. Chem. Res.* **1987**, *20*, 408.
(3) Poliakoff, M. *Spectrochim. Acta* **1987**, *43A*, 217.
(4) Ryther, R. J.; Weitz, E. *J. Phys. Chem.* **1991**, *95*, 9841.
(5) Trushin, S. A.; Fuss, W.; Kompa, K. L.; Schmid, W. E. *J. Phys. Chem. A* **2000**, *104*, 1997.
(6) LeadBeater, N. *Coord. Chem. Rev.* **1999**, *188*, 35.
(7) Snee, P. T.; Payne, C. K.; Kotz, K. T.; Yang, H.; Harris, C. B. *J. Am. Chem. Soc.* **2001**, *123*, 2255.
(8) We define a strong coupling solvent as one that reacts with the triplet intermediate on the ultrafast timescale, resulting in the formation of a singlet solvated product.
(9) Kotz, K. T.; Yang, H.; Snee, P. T.; Payne, C. K.; Harris, C. B. *J. Organomet. Chem.* **2000**, *596*, 183.
(10) Siegbahn, P. E. M. *J. Am. Chem. Soc.* **1996**, *118*, 1487.

10.1021/ja010648r CCC: $20.00
Published on Web 06/21/2001

Scheme 2. The Results of the Previous Si−H Activation Mechanistic Studies for a Low-Spin $Cr(CO)_5$ Intermediate and a High-Spin $Fe(CO)_4$ Intermediate

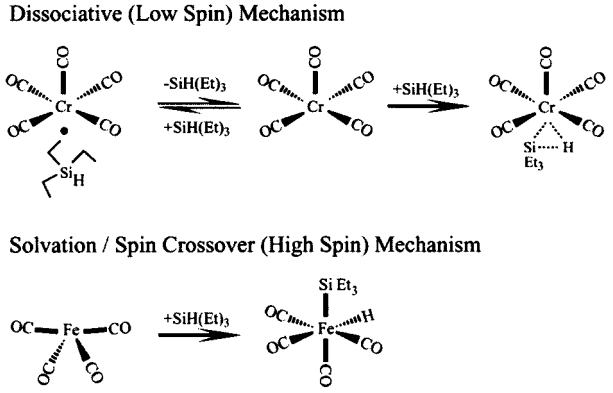

the unusual two carbonyl loss photosubstitution reaction of this species with phosphines. The observation of double CO substitution via a one-photon process is at odds with the conventional belief that only a single carbonyl is lost from an organometallic species following single photon excitation in solution.[11] First observed by Lewis et al.,[12] this reaction was characterized by Nayak and Burkey in a series of elegant mechanistic experiments.[13,14] These authors proposed that the unusual reaction dynamics were due to the formation of triplet $^3Fe(CO)_4$, while other researchers have proposed that the dynamics are due in part to a singlet species.[5] We recently confirmed that $^3Fe(CO)_4$ is formed on the ultrafast timescale in room temperature alkane solution. To resolve this issue, this system has been studied in neat triethylphosphine to develop a comprehensive reaction mechanism for this unusual photosubstitution reaction. The reactivity of the photogenerated species is also investigated using density functional theory, which qualitatively reproduces the trends seen in the experimental data.

II. Methods

Sample Synthesis/Sample Handling. The compounds $Fe(CO)_5$ and triethylphosphine were purchased from Strem and were used without further purification. Methanol, 1-butanol, 1-hexanol, and *tert*-butyl alcohol were purchased from Aldrich. All samples were prepared under nitrogen atmosphere in an airtight, liquid IR flow cell from Harrick Scientific Corporation using a 250 μm cell thickness. The concentration of $Fe(CO)_5$ was approximately 15−25 mM in all solutions.

The compound $Fe(CO)_4(PEt_3)$ was synthesized from $Fe(CO)_5$ and PEt_3 according to the method of Nayak.[15] The sample purity was established using standard spectroscopic methods. The ultrafast spectra of this compound were taken using a 15 mM concentration of $Fe(CO)_4(PEt_3)$ in dry heptane with a 250 μm cell thickness.

Femtosecond Infrared Spectroscopy. Details of the femtosecond IR (fs-IR) spectrometer setup have been published elsewhere.[16] The output of a Ti:sapphire oscillator was amplified in two prism-bored dye-cell amplifiers,[17] which were pumped by the output of a frequency-doubled 30 Hz Nd:YAG laser. The amplified light centered at ~810 nm was then split into three beams. One beam was further amplified to give 70-fs, 7-μJ pulses while the other two were focused into two sapphire windows to generate white light continuum. Desired wavelengths of the white light were selected by two band-pass (BP) filters with full-width-half-maxima (fwhm) of 10 nm, and further amplified by three-stage dye amplifiers to produce light pulses centered at 590 nm as well as 690 nm. In this study, the excitation pulse of 295 nm was generated by frequency doubling the 590-nm light. The resulting UV photons (with energy of ~4 μJ/pulse) were focused into a disk of ~200-μm diameter at the sample to initiate the chemical reactions. The required time delay between a pump pulse and a probe pulse was achieved by guiding the pump beam through a variable delay line.

The broadband, ultrafast probe pulses centered at 5 μm were generated by mixing the 690-nm beam with the 810-nm beam. The resulting ~5 μJ IR pulses having temporal fwhm of about 70 fs (as determined by the duration of the 800 nm beam) and a spectral bandwidth of about 200 cm^{-1} were split into a signal and a reference beam. Both the signal beam and the reference beam were then focused into an astigmatism-corrected spectrographic monochromator to form two spectrally resolved images on a focal-plane-array (FPA) detector, consisting of an engineer grade, 256 × 256-element HgCdTe (MCT) sensing chip. The typical spectral and temporal resolutions for this setup are 4 cm^{-1} and 300 fs, respectively. The polarizations of the pump and the probe pulse were set at the magic angle (54.7°) to ensure that all signals were due to population dynamics. A broad, wavelength-independent background signal from CaF_2 windows has been subtracted from the transient spectra and kinetic traces.

Quantum Chemical Modeling. To compare single point energies consistently, all calculations were carried out using DFT optimized geometries. The hybrid B3LYP functional was used for the DFT calculations with the Jaguar package.[18−20] The basis set consisted of the 6-31G** basis functions for H, C, O, and P[21,22] and the Los Alamos Effective Core Potential (ECP) for Fe with the outermost core orbitals included in the valence description.[23] All geometry optimizations were followed by a frequency analysis to make certain that the optimized geometries were at a minimum. The coupling (spin−orbit) strengths of the proposed triplet intermediates were calculated at the ground-state triplet geometries using casscf optimized wavefunctions,[24] with the GAMESS-US package.[25] As it is computationally unfeasible to calculate the full Breit−Pauli spin−orbit Hamiltonian for the optimized casscf wavefunction, the two-electron component of the operator is removed and an approximate metal charge (Z_{eff}) is used. The Z_{eff} at the metal center described by Koseki et al. was used to calculate the spin−orbit coupling using the lanl2dz basis set.[26]

For computational efficiency, the neat PEt_3 interaction with the singlet organometallic complexes was modeled using $P(CH_3)_3$. Likewise, the alcohol interaction calculations use CH_3OH as a model. The bond strengths of the ground-state species were also calculated at the DFT/B3LYP level of theory using the counterpoise method to account for basis set superposition error[27,28] including zero point energy (ZPE) corrections. The ΔE for the reactions

$$P(CH_3)_3 + {}^3Fe(CO)_4 \rightarrow {}^3Fe(CO)_3[P(CH_3)_3] + CO \qquad (1)$$

and

(11) This is a result of vibrational relaxation of the initially hot photoproduct in the solvent bath. See ref 15 and references therein.

(12) Lewis, J.; Nyholm, R. S.; Sandhu, S. S.; Stiddard, M. H. B. *J. Chem. Soc.* **1964**, 2825.
(13) Nayak, S. K.; Burkey, T. J. *J. Am. Chem. Soc.* **1993**, *115*, 6391.
(14) Nayak, S. K.; Farrell, G. J.; Burkey, T. J. *Inorg. Chem.* **1994**, *33*, 2236.
(15) Nayak, S. K.; Burkey, T. J. *Inorg. Chem.* **1992**, *31*, 1125.
(16) Lian, T.; Bromberg, S. E.; Asplund, M. C.; Yang, H.; Harris, C. B. *J. Phys. Chem.* **1996**, *100*, 11994.
(17) Bethune, D. S. *Appl. Opt.* **1981**, *20*, 1987.
(18) Becke, A. D. *J. Chem. Phys* **1993**, *98*, 5648.
(19) Lee, C.; Yang, W.; Parr, R. G. *Phys. Rev.* **1988**, *B41*, 785.
(20) Stephens, P. J.; Devlin, F. J.; Chabalowski, C. F.; Frisch, M. J. *J. Phys. Chem.* **1994**, *98*, 11623.
(21) Hehre, W. J.; Ditchfield, R.; Pople, J. A. *J. Chem. Phys.* **1972**, *56*, 2257.
(22) Francl, M. M.; Petro, W. J.; Hehre, W. J.; Binkley, J. S.; Gordon, M. S.; Defrees, D. J.; Pople, J. A. *J. Chem. Phys.* **1982**, *77*, 3654.
(23) Hay, P. J.; Wadt, W. R. *J. Chem. Phys.* **1985**, *82*, 299.
(24) The method used optimized ground-state core orbitals for the ground- and excited-state casscf optimization. See: Lengsfield, B. H.; Jafri, J. A.; Phillips, D. H. *J. Chem. Phys.* **1981**, *74*, 6849.
(25) Schmidt, M. W.; Baldridge, K. K.; Boatz, J. A.; Elbert, S. T.; Gordon, M. S.; Jensen, J. H.; Koseki, S.; Matsunaga, N.; Nguyes, K. A.; Su, S.; Windus, T. L.; Dupuis, M.; Montgomery, J. A. *J. Comput. Chem.* **1993**, *14*, 1347.
(26) Koseki, S.; Schmidt, M. W.; Gordon, M. S. *J. Phys. Chem. A* **1998**, *102*, 10430.
(27) Boys, S. F.; Bernardi, F. *Mol. Phys.* **1970**, *19*, 553.
(28) Liu, B.; McLean, A. D. *J. Chem. Phys.* **1973**, *59*, 4557.

$$HOCH_3 + {}^3Fe(CO)_4 \rightarrow {}^3Fe(CO)_3[HOCH_3] + CO \qquad (2)$$

were also calculated as $\Delta E = E_{products} - E_{reactants} + \Delta ZPE$.

To describe the trends seen in the reactivity of the triplet species $^3Fe(CO)_4$ in alcohol solution, the DFT potential energy curves for the singlet and triplet $Fe(CO)_4$ with $HOCH_3$ were calculated by fixing the metal−O bond lengths of the organometallic complex and optimizing the remaining geometric parameters. Likewise the DFT potential surfaces for $Fe(CO)_4$ and $Fe(CO)_3(PEt_3)$ in triethylphosphine were calculated using fixed Fe−P bond lengths with $Fe(CO)_3P(CH_3)_3$ and $P(CH_3)_3$ as model complexes. This was done for both singlet and triplet organometallic fragments near the singlet−triplet crossing region. This type of analysis builds an approximate potential energy surface for the bond activation reaction as a function of the Fe−X (X = P, O) distance, although the actual activation coordinate is more complex due to the high dimensionality of the dynamics.

III. Results

The infrared spectra in the CO stretching region are presented in the form of difference absorbance spectra in which positive bands indicate the appearance of new species while negative bands (bleaches) represent the depletion of parent molecules. Gaps appear in some spectra where the parent compound has strong absorptions as very little IR signal penetrates the sample in these frequency regions.

A. Photolysis of $Cr(CO)_6$ and $Fe(CO)_5$ in Neat Alcohol Solution. The time-resolved spectra of $Fe(CO)_5$ in *tert*-butyl alcohol are shown in Figure 1. At early times the spectra of the triplet species appear broad and highly overlapped with parent hot bands. At later times the triplet species decays to form the singlet hydroxyl solvated $Fe(CO)_4(HO-R)$ product with peak positions at 1950 and 2047 cm^{-1}.[29] The spectra in other alcohol solvents are qualitatively similar. The kinetic traces of the formation of the singlet hydroxyl solvated products in all the alcohol solvents are shown in Figure 2 and are summarized in Table 1 and Scheme 3A.

The rearrangement timescales of singlet $^1Cr(CO)_5$ to form the hydroxyl solvated products $Cr(CO)_5(OH-R)$ in methanol, 1-butanol and 1-hexanol are given in Table 1. Also listed are the solvent's viscosities. Overall, the rearrangement time scales are much longer than those observed for the iron complexes.

B. Photolysis of $Fe(CO)_5$ in Neat PEt_3 Solution. In neat triethylphosphine solution, the single substituted photoproduct $Fe(CO)_4PEt_3$ absorbing at 1932, 1969, and 2047 cm^{-1} appears on a time scale of 50 ps and remains constant to 660 ps as shown in Figure 3.[30] Also appearing in the spectra is an unknown intermediate absorbing at 1908 cm^{-1}, which decays in 2.8 ± 0.5 ns with the concomitant formation of the disubstituted $Fe(CO)_3(PEt_3)_2$ peak at 1870 cm^{-1}. The kinetic trace of the decay of the unknown intermediate is shown in Figure 4. The single substituted $Fe(CO)_4PEt_3$ and disubstituted $Fe(CO)_3(PEt_3)_2$ products are identified by comparing the vibrational frequencies with the literature values.[31,32] The rise times of $Fe(CO)_4PEt_3$ and the unknown intermediate species may be attributed to vibrational relaxation of the initially hot photoproduct confirmed by the slight narrowing and blue shifting of the photoproduct peak at early times.[33−35]

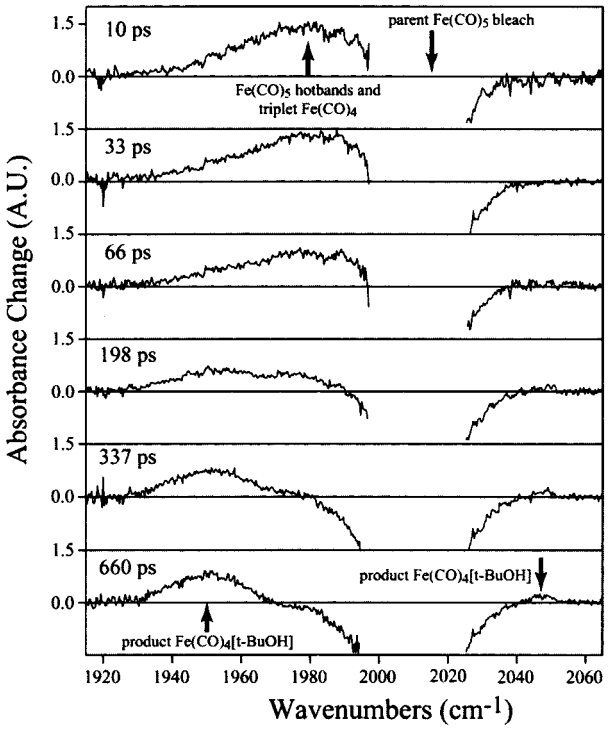

Figure 1. Transient difference spectra in the CO stretching region for $Fe(CO)_5$ in neat *tert*-butyl alcohol at 10, 33, 66, 200, 340, and 660 ps following 295-nm UV photolysis. (A.U. = arbitrary unit ~ 0.01 OD.)

Shown in the inset of Figure 3 is the difference spectrum of the single substituted product $Fe(CO)_4PEt_3$ in heptane solution taken upon photolysis at 295 nm. A single species appears absorbing at 1911 cm^{-1}, which coincides with the unknown intermediate peak seen in the $Fe(CO)_5$/neat PEt_3 data. These data are used in the assignment of the unknown intermediate species, given in the Discussion.

C. DFT and ab Initio Calculation Results. Theoretical calculations have been used to characterize the nature of the transient intermediates under study. The purpose of these calculations is to establish the ground spin state of the intermediates and to understand the trends seen in the reactivity of these species.

Geometry Optimization. Shown in Figure 5 are the ground-state geometries and relevant geometric parameters of $^1Fe(CO)_4(HOCH_3)$, $^1Fe(CO)_4P(CH_3)_3$, $^3Fe(CO)_3P(CH_3)_3$, and $^1Fe(CO)_3[P(CH_3)_3]_2$. The DFT results for $Fe(CO)_5$ and $^3Fe(CO)_4$ have been published previously.[7] These structures were used in the calculations of ground spin states and ligand binding energies, discussed below.

Energy Calculations. The calculated metal−ligand binding energies as well as spin state energy splittings are listed in Tables 2 and 3, respectively. The DFT results predict a lower energy for the triplet state relative to that of the singlet for $^3Fe(CO)_4$, $^3Fe(CO)_3[P(CH_3)_3]$, and $^3Fe(CO)_3[HOCH_3]$ and as summarized in Table 3. The reaction enthalpy for carbonyl substitution of $^3Fe(CO)_4$ by $P(CH_3)_3$ has been calculated to be +1.4 kcal/mol, while the corresponding substitution by $HOCH_3$ is unfavorable by +14.5 kcal/mol.

To understand the reactivity of these triplet species, the Fe−O (Fe−P) coordinate potential energy curves were calculated at

(29) The product is assigned by the similarity of the spectral positions to those seen in $Fe(CO)_4$(acetonitrile) and $Fe(CO)_4$(*tert*-butyl nitrile). See ref 14.

(30) The 1969 cm^{-1} peak is difficult to see on the scale of the figure. The kinetics for this species was followed at 1932 cm^{-1}.

(31) Van Tentergem, M.; Van Der Kelen, G. P.; Claeys, E. C. *J. Mol. Struct.* **1982**, *80*, 317.

(32) Reckziel, A.; Bigorgne, M. *J. Organomet. Chem.* **1965**, *3*, 341.

(33) Dougherty, T. P.; Heilweil, E. J. *Chem. Phys. Lett.* **1994**, *227*, 19.

(34) Dougherty, T. P.; Grubbs, W. T.; Heilweil, E. J. *J. Phys. Chem.* **1994**, *98*, 9396.

(35) Dougherty, T. P.; Heilweil, E. J. *J. Phys. Chem.* **1996**, *100*, 201.

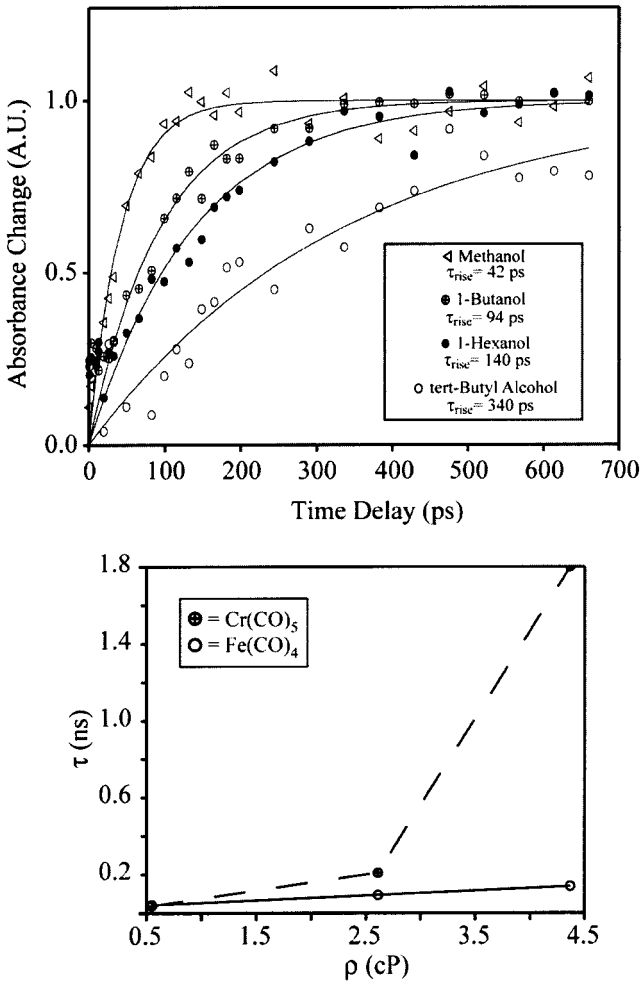

Figure 2. The kinetics of the formation of the singlet OH-solvated product in the reaction of $Fe(CO)_4$ in various alcohol solutions. Also shown are the product formation lifetimes of $Fe(CO)_4$ and $Cr(CO)_5$ in linear alcohols as a function of solvent viscosity.

Table 1. The Timescales of Formation of the OH-Solvated Singlet Intermediate for the Photochemical Reaction of $Fe(CO)_5$ and $Cr(CO)_6$ in Various Alcohols (The $Fe(CO)_5$ Results Approximately Scale with the Solvent Viscosity, See Text)

	methanol (ps)	*n*-butanol (ps)	*n*-hexanol (ps)	*tert*-butyl alcohol (ps)
solvent viscosity[a]	0.55	2.61	4.37	5.88
τ, $^3Fe(CO)_4$	42.3[b]	93.7	138	335
τ, $^1Cr(CO)_5$	38[b]	209	1800	–

[a] The viscosity in units of centipoise, from ref 50. [b] In methanol, the alkyl-solvated $Cr(CO)_5$ or high-spin $Fe(CO)_4$ intermediates are not observed. Consequently, the kinetics are likely due to cooling of the final photoproduct which forms at a faster rate. In fact, Simon et al. observed a time scale of 2.5 ps for the formation of $Cr(CO)_5(HOCH_3)$ in their earlier visible wavelength study.[51]

the DFT level of theory. The results are shown in Figure 6 and are summarized in Table 4. Overall, the results show that there exist a small attractive interaction between $^3Fe(CO)_4$ and $HOCH_3$ and $P(CH_3)_3$ of −3.02 and −0.6 kcal/mol, respectively. The singlet/triplet crossover points occur at potentials of −3.01 and −0.31 kcal/mol, respectively, below the (unsolvated) triplet ground-state energy due to these attractive interactions. While the data show that the interaction of $^3Fe(CO)_3P(CH_3)_3$ with $P(CH_3)_3$ has a local minimum, this complex is unstable with respect to the isolated fragments by +4.2 kcal/mol. As a result, the singlet/triplet crossover point for $Fe(CO)_3P(CH_3)_3 + P(CH_3)_3$

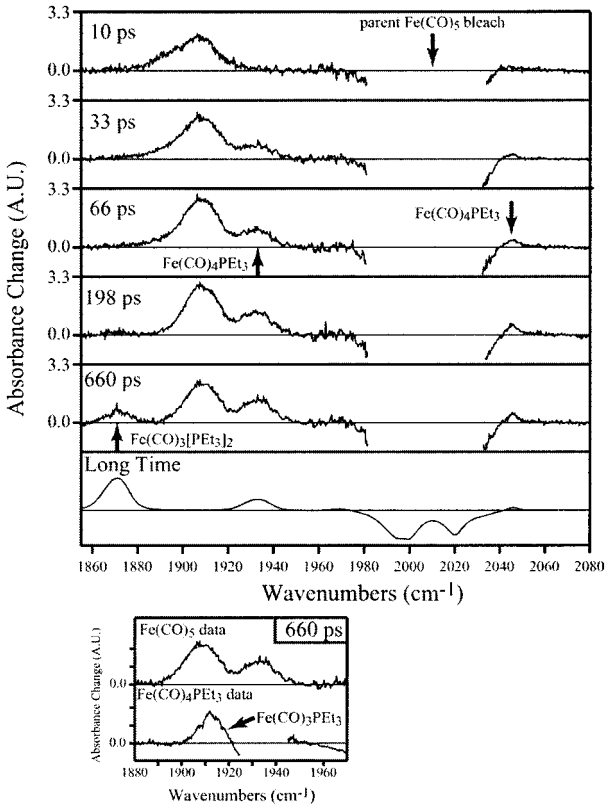

Figure 3. Transient difference spectra in the CO stretching region for $Fe(CO)_5$ in neat triethylphosphine at 10, 33, 66, 200, and 660 ps following 295-nm UV photolysis. The last panel shows the long time difference spectrum. The relative peak heights in the long time spectrum are probably affected by secondary photolysis. The inset is the spectrum from the photolysis of $Fe(CO)_4P(CH_3)_3$ in heptane solution. (A.U. = arbitrary unit ~ 0.01 OD.)

Scheme 3. The Substitution Mechanisms of Photogenerated $^3Fe(CO)_4$ in Alcohol and Triethylphosphine Solutions

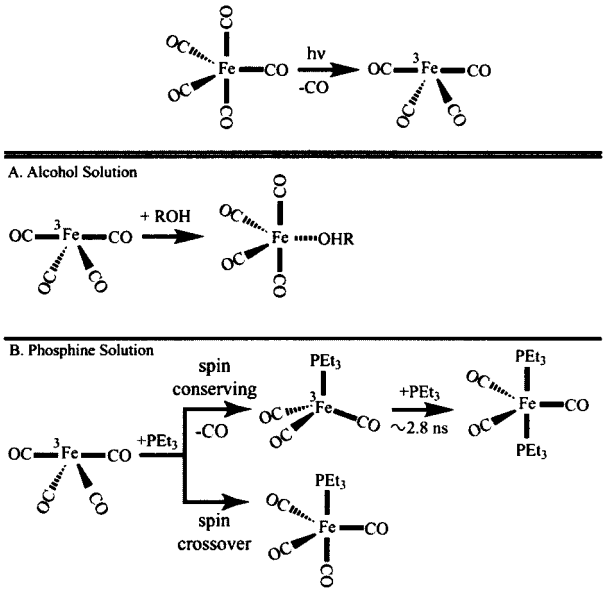

occurs at a potential of +4.53 kcal/mol above that of the unsolvated species. Overall, there does not appear to be a significant attractive interaction between triplet $^3Fe(CO)_3P(CH_3)_3$ and $P(CH_3)_3$.

Spin−orbit coupling (SOC) calculations at the ground state triplet geometry were also performed using the optimized

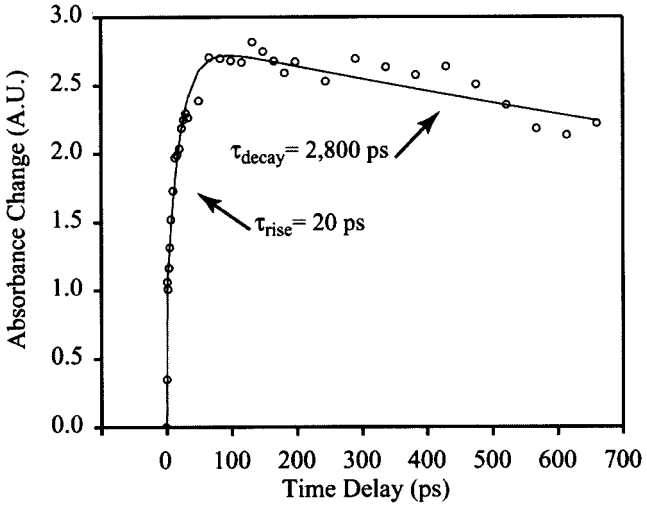

Figure 4. The kinetics of the decay of the $^3Fe(CO)_3PEt_3$ intermediate in neat triethylphosphine. See text.

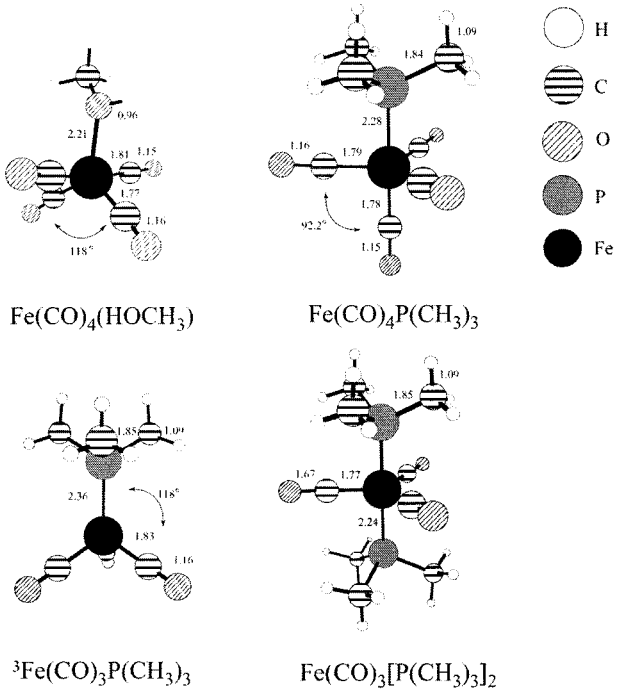

Figure 5. Geometries of the parent molecule, the triplet intermediate, and the final products optimized at the DFT/B3LYP level of theory. The bond lengths are in Å and the angles are in deg.

Table 2. The Binding Strengths of Various Organometallic Species with CO and $P(CH_3)_3$

fragment	ligand	ΔE (kcal/mol)
$Fe(CO)_4$	CO[a]	67.3 (ax), 52.2 (eq)
$^1Fe(CO)_4$	$HOCH_3$	13.2
$^1Fe(CO)_4$	$P(CH_3)_3$	46.0
$^3Fe(CO)_4$	$P(CH_3)_3$	1.3
$^3Fe(CO)_3$	$P(CH_3)_3$	28.8
$^1Fe(CO)_3[P(CH_3)_3]$	$P(CH_3)_3$	37.8

[a] From ref 7.

multiconfigurational wavefunction and are summarized in Table 4. The coupling constants are similarly small for $Fe(CO)_4$ and $Fe(CO)_4P(CH_3)_3$, and for the most part the observed dynamics appear to follow the trend in the calculated singlet/triplet spin crossing barriers.

Table 3. The Energetic Splitting between Singlet and Triplet States at Various Levels of Theory

(ground state)-organometallic	ΔE^a (DFT) (kcal/mol)	vert.-ΔE^b (DFT) (kcal/mol)
(triplet)-$Fe(CO)_4$	5.43[c]	22.9
(triplet)-$Fe(CO)_3P(CH_3)_3$	6.31	29.3
(triplet)-$Fe(CO)_3(HOCH_3)$	3.09	27.7

[a] Calculated as E(singlet) − E(triplet). [b] The ΔE between the ground and excited spin state at the ground-state geometry. [c] From ref 7.

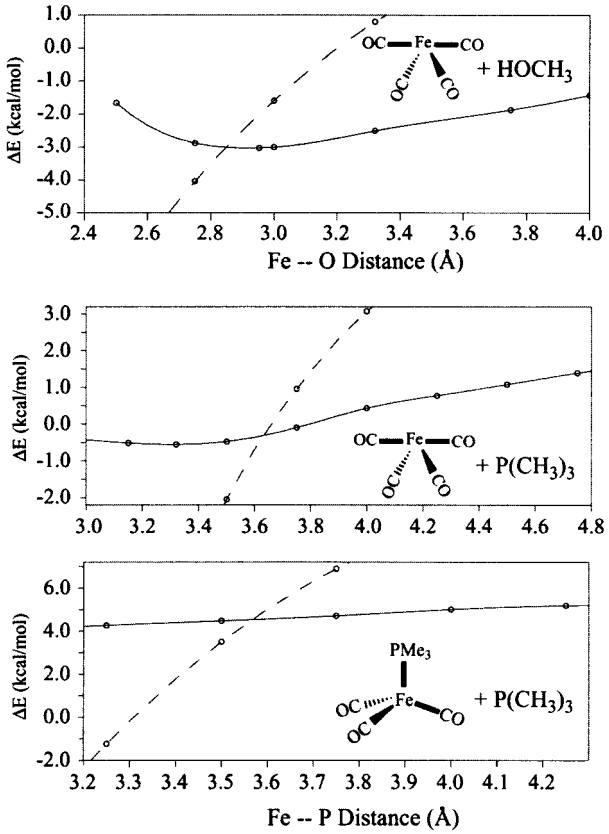

Figure 6. The results of the DFT singlet and triplet organometallic/$HOCH_3$ and $P(CH_3)_3$ energy calculations. The curves are generated by performing a geometry optimization at a fixed Fe−(P or O) bond length for each organometallic system. The singlet potential curves are represented by dashed lines and the triplet curves have solid lines. The lines are spline fits to the data (circles) and are presented for visualization purposes only.

IV. Discussion

A. Liquid-Phase Photolysis of $Fe(CO)_5$ in Alcohol Solution. The spectra of $Fe(CO)_5$ in *tert*-butyl alcohol solution are shown in Figure 1. We have previously established that the major product formed upon photolysis of $Fe(CO)_5$ in alkane and silane solutions is the triplet species $^3Fe(CO)_4$.[7] As such, at early times the spectral features appear to be due to triplet $^3Fe(CO)_4$ peaks which are broadened and possibly overlapped with both parent $Fe(CO)_5$ and triplet $^3Fe(CO)_4$ hot bands. These bands later decay with the concomitant formation of the singlet hydroxyl solvated product species $^1Fe(CO)_4(HO-R)$. As summarized in Table 1 and Figure 2, the kinetics of the formation of the singlet hydroxyl solvated products are generally faster than observed in the $^1Cr(CO)_5$ studies and scale linearly with solvent viscosity. The same linear trend is not observed in the chromium data.[36] These results are consistent with the formation of intermediates in different spin states. Previous theoretical reports have shown that triplet organometallic species do not have strong interactions

Table 4. The Results of the DFT Potential Energy Curve Calculations as Well as a Summary of the Singlet/Triplet Spin−Orbit Couplings and the Triplet Species Lifetimes in Solution

complex/model solvent	min (Å)[a]	interaction *E* (kcal/mol)[b]	singlet/triplet crossover (Å)[c]	barrier (kcal/mol)[d]	SOC (cm^{-1})	τ (ps)
$Fe(CO)_4/CH_3OH$	2.92	−3.02	2.85	−3.01	2.6	<42
$Fe(CO)_4/P(CH_3)_3$	3.30	−0.6	3.63	−0.31	2.6	<50
$Fe(CO)_4P(CH_3)_3/P(CH_3)_3$			3.57	4.53	36	2800

[a] The Fe−O (Fe−P) distance at a local minimum. [b] The well depth at the local minimum. [c] The Fe−O (Fe−P) distance where the singlet and triplet curves cross. [d] The energy at the singlet/triplet crossover.

with alkanes.[10,37−40] Thus triplet $^3Fe(CO)_4$ should not interact with the alkyl group of the solvent, and yet will react upon encountering the strong coupling hydroxyl group and quickly cross over to the hydroxyl solvated singlet state. As a result, the reaction timescale is essentially diffusion controlled and should have a linear viscosity dependence.[41] The singlet species $Cr(CO)_5$ has stronger interactions with alkanes and the kinetics are dominated by the dissociation time scale of an alkyl/$Cr(CO)_5$ complex.[9,42,43] These results are also consistent with Poliakoff and Turner's earlier observation that $Cr(CO)_5$ is more reactive toward alkanes.[1] Consequently, the strength of the metal−alkyl interaction as well as the number of alkyl sites will dominate the rearrangement timescales for this singlet intermediate.[44]

B. Liquid-Phase Photolysis of $Fe(CO)_5$ in Triethylphosphine Solution. In triethylphosphine, the triplet $^3Fe(CO)_4$ photoproduct is not directly observed. Instead, the spectra in Figure 3 show the fast formation of $Fe(CO)_4PEt_3$ and an unknown intermediate at 1908 cm^{-1}. While $Fe(CO)_4PEt_3$ concentration appears constant to 660 ps, the intermediate at 1908 cm^{-1} appears to decay in 2.8 ± 0.5 ns with the concomitant formation of the double substituted product $Fe(CO)_3(PEt_3)_2$ absorbing at 1870 cm^{-1}.

Considering that the unknown intermediate and the disubstituted product are kinetically coupled, the identity of the intermediate is proposed to be $^3Fe(CO)_3PEt_3$ and is supported by spectroscopic evidence. As seen in Figure 3, the intermediate $^3Fe(CO)_3PEt_3$ formed upon photolysis of $Fe(CO)_4PEt_3$ in heptane solution absorbs at 1911 cm^{-1}, and no other absorptions attributed to this species are observed.[45] With the fact that the absorption frequency of this species is similar to that observed in the $Fe(CO)_5$/triethylphosphine study and the DFT calculations have established the triplet species is the ground state, we are led to the conclusion that the intermediate is $^3Fe(CO)_3PEt_3$. This result is also consistent with the previously reported mechanism.[13,14] These results are summarized in Scheme 3B.

With the identity of the double-CO substitution intermediate in mind, a mechanism for the phosphine-substitution reaction may be proposed. Our previous investigation has shown that upon photolysis of $Fe(CO)_5$ in solution, a single carbonyl is lost and the photoproduct is in the unsolvated ground triplet state.[7] In neat triethylphosphine solution, the initial reaction of $^3Fe(CO)_4$ with PEt_3 is divided into two parallel channels. There exists a concerted process in which a second carbonyl is lost and the $^3Fe(CO)_3PEt_3$ intermediate is formed, which is overall spin conserving. This species then reacts with PEt_3 to form the final disubstituted product $^1Fe(CO)_3(PEt_3)_2$. There also exists a spin nonconserving channel for reaction of $^3Fe(CO)_4$ with PEt_3 to form $^1Fe(CO)_4PEt_3$, which is chemically inert to substitution at room temperature.[46] The proposed mechanism is qualitatively similar to that previously reported; however, the present study finds no spectroscopic evidence for the formation of $^3Fe(CO)_4PEt_3$ or $^1Fe(CO)_4$ as precursors to $^1Fe(CO)_4PEt_3$ or $^3Fe(CO)_3PEt_3$.[47] As a previous account suggests that $Fe(CO)_5$ also undergoes photochemical disubstitution reactions with olefins,[48] the spin conserving/nonconserving reaction to form monosubstituted and disubstituted products appears to be a more general phenomena.

C. Understanding the Trends of Reactivity. While it has been shown that triplet $^3Fe(CO)_4$ is stable to 660 ps in alkane solution,[7] this intermediate reacts on a fast (ps) timescale in alcohol and triethylphosphine solution. Although triplet $^3Fe(CO)_4$ is very reactive, the triplet intermediate $^3Fe(CO)_3PEt_3$ reacts in triethylphosphine on a much longer (ns) timescale. The experimental results may be interpreted in terms of the barrier at the singlet/triplet curve crossover and the similarity of the calculated coupling constants for the singlet and triplet surfaces.

The trends in the reactivity of these species are elucidated through the approximate nonadiabatic potential energy surfaces generated by the DFT singlet and triplet organometallic/model ligand calculations in Figure 6.[49] The singlet state (dashed) curves for all the species slope downhill with decreasing Fe−O (Fe−P) distance, which shows that the singlet substituted product is overall the most favorable species energetically. These theoretical calculations explain the fast reactivity of triplet $Fe(CO)_4$ in alcohol and triethylphosphine solution. This system appears to have no classical barrier to the reaction due to the attractive interactions between $^3Fe(CO)_4$ species with $HOCH_3$ and $P(CH_3)_3$. The triplet species Fe−O (Fe−P) minima are on the order of 1 Å from the singlet activated product bond length, which indicates that only a slight rearrangement is necessary

(36) The data for the linear alcohols are used. For the $Fe(CO)_4$ lifetimes vs viscosity in linear alcohols, a linear fit has $r^2 > 0.99$. In the case of *tert*-butyl alcohol, the product formation time scale is longer than expected based solely on viscosity; however, the difference is likely due to steric factors which we have not taken into account.

(37) Bengali, A. A.; Bergman, R. G.; Moore, C. B. *J. Am. Chem. Soc.* **1995**, *117*, 3879.

(38) Blomberg, M. R. A.; Siegbahn, P. E. M.; Svensson, M. *J. Am. Chem. Soc.* **1992**, *114*, 6095.

(39) Siegbahn, P. E. M.; Svensson, M. J. *J. Am. Chem. Soc.* **1994**, *116*, 10124.

(40) Carroll, J. J.; Weisshaar, J. C.; Haug, K. L.; Blomberg, M. R. A.; Siegbahn, P. E. M.; Svensson, M. *J. Phys. Chem.* **1995**, *99*, 13955.

(41) Steinfeld, J. I.; Francisco, J. S.; Hase, W. L. *Chemical Kinetics and Dynamics*; Prentice-Hall: Englewood Cliffs, NJ, 1989.

(42) Ladogana, S.; Nayak, S. K.; Smit, J. P.; Dobson, G. R. *Inorg. Chem.* **1997**, *36*, 650.

(43) Burkey, T. J. *J. Am. Chem. Soc.* **1990**, *112*, 8329.

(44) We are presently developing a stochastic model to describe the results seen in our rearrangement data, see ref 9.

(45) The compound $Fe(CO)_4PEt_3$ is known to lose one carbonyl upon photolysis to form $Fe(CO)_3PEt_3$. See ref 15.

(46) Cardaci, G. *Inorg. Chem.* **1974**, *13*, 368.

(47) Our proposed mechanism is fully consistent with that previously reported in ref 14, if one simply removes the existence of $^3Fe(CO)_4PEt_3$.

(48) Angermund, H.; Bandyopadhyay, A. K.; Grevels, F.-W.; Mark, F. *J. Am. Chem. Soc.* **1989**, *111*, 4656.

(49) A method has recently been developed by another group to calculate the exact barrier heights at the spin crossing point. See for example: Harvey, J. N. *J. Am. Chem. Soc.* **2000**, *122*, 12401.

(50) Prausnitz, J. M.; Reid, R. C. *The Properties of Gases and Liquids*, 4th ed.; McGraw-Hill: New York, 1987.

(51) Simon, J. D.; Xie, X. *J. Phys. Chem.* **1986**, *90*, 6751.

to form the product. Although the spin−orbit strength of $Fe(CO)_4$ is calculated to be very small, the low classical barrier, as well as triplet−solvent interactions, elucidates why such a fast reaction occurs between $^3Fe(CO)_4$ and alcohols and triethylphosphine.

There does not appear to be an attractive interaction of triplet $^3Fe(CO)_3P(CH_3)_3$ with $P(CH_3)_3$, resulting in a larger classical reaction barrier. The spin−orbit strengths of $^3Fe(CO)_3P(CH_3)_3$ and $^3Fe(CO)_4$ are comparably low, and as a result the longer timescale of this reaction compared to $^3Fe(CO)_4 + P(CH_3)_3$ follows the trend in the calculated classical barriers. It is interesting to note that there is no evidence for disubstitution in alcohol solution. Unfortunately, we have not been able to calculate the transition state structures within the triplet manifold for these disubstitution reactions with certainty. It is interesting to note, however, that the DFT enthalpy results show that carbonyl substitution of $^3Fe(CO)_4$ by $P(CH_3)_3$ is energetically unfavorable by only +1.4 kcal/mol. In contrast, the calculated ΔE for carbonyl substitution of $^3Fe(CO)_4$ by $HOCH_3$ is an order of magnitude larger.

V. Conclusion

We have shown that the photochemical dynamics of $Fe(CO)_5$ are consistent with triplet state reactivity. Several previous studies have shown that this species has weak interactions with alkane solvents.[10,37−40] As a result, the alcohol solvents are best viewed as viscous media through which the coordinatively unsaturated $^3Fe(CO)_4$ intermediates diffuse. This effect is seen in the reactivity of $^3Fe(CO)_4$ in various alcohol solvents in which the kinetics of product formation scale linearly with the inverse of the solvent viscosity. These results are in contrast with the dynamics of the singlet intermediate $^1Cr(CO)_5$, which has a very complex interaction with the solvent environment. Specifically, the rate of reaction of $^1Cr(CO)_5$ with alcohols is slowed by the coordination of the alkyl moiety of the solvent which serves to impede the coordination of the metal center with the hydroxyl group.

The observation of a two carbonyl photosubsitiution by $Fe(CO)_5$ has been shown to be a result of the parallel partitioning of the reaction pathway into spin conserving and spin forbidden reaction channels. Contrary to previous reports, there is no evidence for the participation of a singlet intermediate or a high-spin solvated complex in the reaction mechanism. Overall, the theoretical methods employed in this paper greatly assist our understanding of these transient intermediates, which have lifetimes too short for conventional characterization. These results indicate that the reaction timescales follow the trends seen in the calculated classical reaction barriers, given similar singlet−triplet coupling constants.

Acknowledgment. This work was supported by a grant from the National Science Foundation. We also acknowledge equipment used under the Office of Basic Energy Science, Chemical Science Division, U.S. Department of Energy contract DE-AC03-76SF00098. We would like to thank Mr. Edmundo Angeles for the use of a FTIR spectrometer.

JA010648R